

MDPI

Article

Spatial and Temporal Variation in Wave Overtopping Across a Coastal Structure Based on One Year of Field Observations

Jennifer Brown ^{1,*}, Gerd Masselink ², Margaret Yelland ¹, Christopher Stokes ², Timothy Poate ², Robin Pascal ¹, David Jones ³, John Walk ¹, Christopher Cardwell ¹, Barry Martin ³, Peter Ganderton ², Julie Gregory ⁴, Ruth Adams ⁵ and Joseff Saunders ^{2,5}

- ¹ National Oceanography Centre, European Way, Southampton SO14 3ZH, UK
- School of Biological and Marine Sciences, University of Plymouth, Drake Circus, Plymouth PL4 8AA, UK
- National Oceanography Centre, Joseph Proudman Building, 6 Brownlow Street, Liverpool L3 5DA, UK
- ⁴ Network Rail Wales & Western Region, Western House, 1 Holbrook Way, Swindon SN1 1BD, UK
- South West Coastal Monitoring, Teignbridge District Council, Forde House, Newton Abbot TQ12 4XX, UK
- Correspondence: jebro@noc.ac.uk

Abstract

Coastal managers worldwide must prepare for changes in annual wave overtopping events due to climate change and sea-level rise. Research often assesses overtopping discharges by extreme events at a sea wall crest, typically using data from physical models or empirical rules based on scaled experiments. Here, we analyse a unique 1-year field dataset of coastal wave overtopping, from SW England, to determine the number of individual waves, regardless of their size, overtopping two locations across a coastal structure. The coastal conditions causing the most frequent overtopping differ from those driving it landward, complicating hazard communications for multiuse infrastructure. These data are the first field observations covering a year of tide, wave and wind conditions that cause overtopping of a vertical sea wall. Storms have a minimal (<2%) contribution to the number of tides associated with overtopping and the prevailing wave direction was not that associated with most overtopping events. Overtopping histograms identify the variability in the most likely time of overtopping relative to high tide for different wave categories across the structure. Sea-level rise, beach lowering and climate change will influence the annual number of waves overtopping in future. Change will be a complex balance between overtopping by different wave categories due to their likelihood of coincidence with water levels that do not cause depth-limitation over the foreshore or (partial-)reflection off the structure. It is possible the number of waves overtopping will reduce at the crest of a sea wall, while more of those overtopping waves will travel further inland.

Keywords: coastal wave overtopping; coastal hazard monitoring; coastal hazard management; climate impact; storm impact; sea-level rise; landward wave overtopping distribution

check for **updates**

Academic Editor: Rosaria Ester Musumeci

Received: 17 October 2025 Revised: 5 November 2025 Accepted: 13 November 2025 Published: 18 November 2025

Citation: Brown, J.; Masselink, G.; Yelland, M.; Stokes, C.; Poate, T.; Pascal, R.; Jones, D.; Walk, J.; Cardwell, C.; Martin, B.; et al. Spatial and Temporal Variation in Wave Overtopping Across a Coastal Structure Based on One Year of Field Observations. J. Mar. Sci. Eng. 2025, 13, 2194. https://doi.org/10.3390/ jmse13112194

Copyright: © 2025 by the authors. Licensee MDPI, Basel, Switzerland. This article is an open access article distributed under the terms and conditions of the Creative Commons Attribution (CC BY) license (https://creativecommons.org/licenses/by/4.0/).

1. Introduction

Wave overtopping at the coastline occurs as a flow of water or vertical plume of spray travelling landward over the crest (highest point) of a coastal barrier or structure (natural or engineered). To reduce the annual deaths due to wave overtopping incidents in Europe, research specifically into understanding tolerable and permissible wave overtopping limits increased in momentum with the UK VOWS and EU CLASH projects [1]. Mean discharge, peak volumes and flood area are often used to assess flood damages; however, for safety

people also need to be aware of their likely exposure [2]. Overtopping limits for different safety requirements (e.g., pedestrians, vehicles) will vary for different structures due to the horizontal trajectory of the overtopping [3] and the infrastructure use. Preparedness for an overtopping wave will also change the tolerable hazard threshold [1]. With accelerating sealevel rise, changing coastal climate impacts and growth in coastal population, infrastructure and amenities, it is critical to be able to revalidate/calibrate site-specific hazard thresholds and reassess coastal infrastructure protection levels. Field data are urgently required for coastal hazard managers to understand the predictable quantitative hazard conditions relative to local hazard perception (public or infrastructure operators). Understanding the inland variation in overtopping hazard is also critical to clearly communicate cross-structure variability in risks where there are multiuse structures, e.g., public access alongside industry.

Wave overtopping poses a coastal hazard not only by transporting water landward but also by carrying debris from the beach inland. Hazard management, both public and within industry, is required to deliver resilience to damages (physical, economic and social) from flooding and direct impact. Safety measures and mitigation strategies (for people, transport and structures, etc.) must consider both intensity, duration and frequency of overtopping events. Engineered beach-structure designs do not prevent all possible overtopping conditions [4]. While the processes causing overtopping are well understood and standardised [5], it is still critical to understand the site-specific present-day water levelwave-wind regime that contributes most to overtopping hazard. Such information helps to better prepare management activities (coastal structure design/maintenance and early warning systems) for future changes in condition combinations that a location is exposed to. Understanding the exposure of different elements (pedestrians, transport, property, etc.) across a location to wave overtopping is essential for site-specific and element-specific hazard management [4]. Process understanding has typically been gained using controlled physical experiments and numerical simulations which expand the parameter space. While studies focusing on individual wave overtopping hazard are growing, widely used generic hazard thresholds are based on the mean wave overtopping discharge and total volume. As accelerating sea-level rise puts pressure on structure designs, reducing the design life of old structures, there is an increasing need to develop safety strategies in addition to flood management. Interest in understanding additional parameters (e.g., number of waves overtopping, duration of wave overtopping, frequency of wave overtopping and distance of travel inland) is growing. More attention on the wave-by-wave distribution of structure overtopping is required [6]. However, the required data can be difficult to measure or generate in experiments, particularly when run at scale for structures vulnerable to overtopping by plumes of wave spray. Site-specific spatial, i.e., cross-structure, hazard understanding is also needed for multiuse structures. For example, under conditions that do not pose a flood hazard, impact by overtopping spray may still be perceived as dangerous to people or transport and access restricted. Continuous field monitoring collects a wide range of conditions and removes the need to select plausible scenarios to analyse. Information about the wide range of typical conditions driving wave overtopping is thus gained, which is often missed when focusing resource to analyse low probability extreme events, as required for scheme design.

There is a growing concern for coastal cities worldwide about the increasing trend in the occurrence of nuisance (minor but frequent) flooding from multiple drivers, such as rising sea level and compound rainfall with high tide events, as infrastructure ages and urban areas sprawl (e.g., Jeong et al. [7]). Such flooding is increasingly impacting coastal communities, for example, more frequent travel disruption during high tides [8]. In recent decades, the globally averaged number of hours of wave overtopping has increased by 50% [9]. The increasing trend in overtopping hours is projected to be greater than that of

mean sea level with the overtopping hours increasing by a factor of 50 by the end of the 21st century under the highest emissions Representative Concentration Pathway (RCP 8.5) [9]. One third of the global coastline is exposed to direct wave impact considered pertinent for coastal management, with projections indicating a non-linear increase in the number of regions impacted by overtopping in response to global mean sea level [9]. Exposure and vulnerability will be further increased by global population growth [10].

A critical threshold to determine if overtopping will occur and what its nature may be like is the ratio between the barrier/structure's freeboard (the crest elevation above the still water level) and the wave height impacting the barrier/structure at its toe. For vertical structures such as sea walls, common across Europe [11], the water depth and wave steepness at the structure toe are also key parameters, as the wave shoaling and breaking dynamics at the point of impact become important [5]. A flow of water over a vertical structure with a large freeboard is only likely during extreme storm tides, while spray overtopping is more common during typical wavy days with an onshore wind, which often captures public interest [1]. For high vertical beach fronted sea walls, when water levels enable wave breaking directly onto the vertical face a plume of spray can often be sent vertically into the air. An onshore wind component or the onshore wave momentum can carry this plume inland, even against the influence of a recurve or lip if present at the top of the wall. Spray overtopping may also be generated when wind acts on the wave crest, particularly when a reflected wave interacts with an incoming wave close to the structure causing 'clapotti' [2].

For vertical sea walls overtopping can be 'pulsating' or 'impulsive'. The first occurs when the waves are relatively small compared with the water depth and the latter when waves are relatively large compared with the water depth causing them to shoal up over the foreshore or structure and violently break directly onto the structure [2]. Two main wave (spray) overtopping responses occur for vertical beach fronted structures with a large freeboard in consequence to the wave-water level-structure interaction [12,13]: (1) waves are reflected without breaking if the tide creates relatively deep water at the structure toe, causing limited or no overtopping; and (2) waves break directly on to the structure toe causing impulsive loads and (violent/explosive) overtopping. Tides have a major influence on this time-varying interaction as the water depth controls the wave breaking process [5]. Impulsive (violent) overtopping can throw spray high into the air. Nonimpulsive/pulsating (less explosive) overtopping sends less water vertically into the air or may not exceed the structure freeboard for high sea walls. Depending on the local wave-water level regime a vertical structure is exposed to, wave overtopping discharge can be greater during the mid-elevation of a tidal cycle than the highest tidal elevation [11]. How violently the waves break (surging or plunging) onto the structure toe influences the explosiveness of the overtopping. If a wave breaks over the foreshore and there is a low likelihood it will reform, the overtopping is unlikely to be impulsive [11]. Deeper water, due to sea-level rise will reduce the freeboard but could increase or decrease the wave height at the structure toe due to changes in the wave shoaling and breaking dynamics. Changes in the beach profile fronting a structure will also change the wave dynamics (i.e., foreshore breakpoint position, wave steepening prior to breaking and wave reflection off the structure). For a vertical structure with a large freeboard preventing overflow, the change in the shallow water wave dynamics could reduce [11] or slightly increase [14] the overtopping discharge. Sloping structures with low freeboard are at risk of waves overflowing the crest increasing the overtopping discharge [14].

Most hazard forecasting services are based on operational numerical predictions that apply empirical formulae for wave overtopping at a sea wall crest (highest point on the primary structure, e.g., Stokes et al. [15]) to a regional water level-wave forecast and a

recent available beach-barrier/structure profile. Research into wave-by-wave overtopping is mainly conducted through laboratory experiments (e.g., Cecioni et al. [13]) or through numerical prediction to extend the laboratory parameter space (e.g., Bagg et al. [16]) and is limited in the range of wave–structure conditions considered [17]. There is a real need for field observations to capture the full range of conditions and beach-structure profiles under which overtopping occurs and to capture site-specific complexities. In the field 3D complexity, such as oblique and crossing wind and swell waves, occurs. While research in wave-basins (e.g., Van der Werf et al. [18]) is growing, process studies often focus on a single structure type, e.g., dikes or caisson breakwaters. For hazard responders, low energy conditions that cause overtopping have the greatest uncertainty when predicting overtopping due to most attention being given to extreme conditions for scheme design and inundation mapping. These low energy events have a high probability of occurrence each year. Identifying the local coastal drivers of low intensity, high probability events perceived as hazardous for public or safe operations through field observations is crucial for hazard management. Typically, video is used in the field during daylight hours to qualitatively assess wave overtopping to validate numerical predictions (e.g., de Santiago et al. [19]), but emerging technology now enables quantitative monitoring of the occurrence of individual overtopping waves [20]. It is rare to have site-specific field data to develop or calibrate local overtopping predictions (e.g., McGlade et al. [21]). Laboratory experiments are often limited in the range of conditions considered and numerical predictions require site-specific calibration and validation [22]. Thus, forecast uncertainty is introduced, particularly for infrastructure positioned landward of the crest without information about the landward distribution of the overtopping.

To deliver tools for hazard prediction, scheme design and policy development, research has focused on collecting mean overtopping volumes at the crest of a structure. Although important for infrastructure design, limited research has focused on collecting information on the landward distribution of wave overtopping. A relationship between the landward reduction in wave overtopping discharge with distance from the structure crest was proposed based on a UK case study at Samphire Hoe by Pullen et al. [23] and is adopted within the industry standard guidance [5]. Due to the complexity of measuring the inland transport of overtopping waves, later studies have continued to focus on laboratory [24] or numerical approaches [25]. The present field study uses the 'WireWall' measurement system (see Yelland et al. [26] for details) to monitor the individual wave events (plumes of spray, water jets and flow) that travel landward across a coastal structure to create overtopping event histograms for 1-year of data. Here, two WireWalls were deployed across the walkway of a beach fronted vertical sea wall structure, common to Europe, in Dawlish SW England (Figure 1).

Like many countries the UK has a national network of tide gauges, wave buoys and weather stations to monitor environmental conditions. Along with biannual beach surveys, shoreline management plans use these monitoring data to plan hazard management activities and build resilience or adaption plans to climate impacts. Many regions also have an operational flood forecasting service. Across the SW of England, a public Operational Waves and Water Levels (OWWL, ref. [15]) forecast system ingests daily wave and water level forecasts from the Met Office, transforms the conditions along existing survey lines and applies internationally accepted rules [5] to predict overtopping for the range of different beach-structure profiles to issue overtopping hazard warnings. The hazard alerts have been validated using available webcams around the region [15]. Complementing the existing national monitoring and regional prediction service with site-specific observation of wave overtopping enables a frequency distribution of a full year of wave overtopping events to be obtained and understood. This has been achieved using the wave overtopping

research system 'WireWall' [26]. Together the field research and available environmental monitoring allow assessment of how the temporal occurrence of different metocean conditions relative to predicted high tide influence the likelihood of waves overtopping critical landward locations across a coastal structure. Predicted high tide is used as a reference time because it is a readily available parameter to hazard responders and widely used by the public. Dawlish represents a typical beach fronted vertical sea wall to assess the present-day condition drivers of overtopping relative to the standard field datasets available to and used by coastal managers. The data are presented using histograms to provide a frequency distribution to show the variability in number of overtopping wave events relative to different metocean conditions and the time-variability over the high tide cycle. This approach has been used by Scott et al. [28] to assess coastal hazard drivers to support hazard management strategies/response, in their case to rip current incidents.

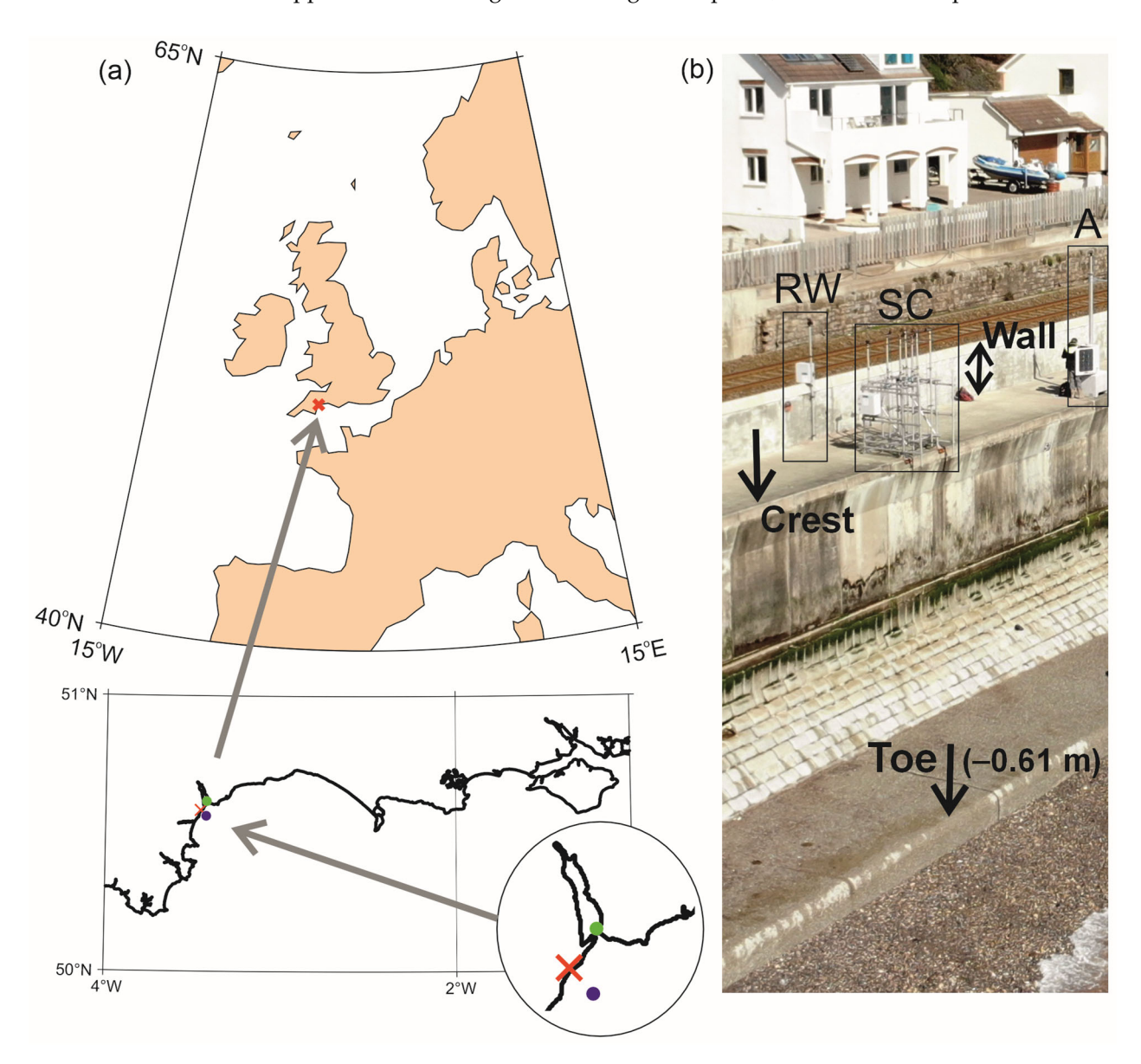


Figure 1. (a) The WireWall study location in Dawlish (X) alongside regional wave (•) and water level monitoring (•) in southwest England (mapping software by Pawlowicz [27]) and (b) the WireWall monitoring systems positioned at the sea wall crest (SC) and railway line wall (RW) adjacent to the anemometer (A). The structure 'toe' elevation is given (in m *OD*) and both the 'crest' representing the highest point of the primary sea wall structure and the secondary 'wall' separating the railway from the pedestrian walkway are identified.

This research provides a field dataset of coastal drivers and consequent overtopping. Focus is given to determining the number of individual waves overtopping, regardless of their magnitude. Analysis of the field data aims to understand the combinations of present-day coastal conditions that cause the most frequent wave overtopping events during a year for a vertical sea wall, using Dawlish SW England as an example. To achieve this a set of objectives have been accomplished:

- 1. Attain and collate a field dataset of concurrent waves, water levels, winds and wave overtopping, to provide valid trigger thresholds of overtopping for local coastal managers (Section 2).
- 2. Identify key drivers that cause most wave overtopping events, both at the sea wall crest and at a distance inland of the crest, for a year of conditions at the field site (Section 3).
- 3. Analyse frequency distributions of a year of wave overtopping events to understand the timing of overtopping relative to the time of predicted high tide (Section 3).
- 4. Propose how the present-day overtopping event distributions could change in future due to sea-level rise and climate impacts on the metocean conditions (Section 4).

2. Methods

To improve wave overtopping hazard forecasting and understanding of the cross-structure distribution of wave overtopping events relative to predicted high tide for vertical sea walls, a year of field data were collected at Dawlish, SW England (Figure 1a). These data complement existing coastal monitoring and numerical prediction. Using histogram analysis quantifies how often (frequently) the existing monitoring or forecast data are associated with wave overtopping events for different condition categories and quantify (count) how many individual waves overtop during set time intervals relative to the time of predicted high tide. All elevations and heights are referenced to Ordnance Datum (Newlyn in the UK), *OD*, the standard for defining Mean Sea Level used by the Ordnance Survey on national mapping and mapping used by coastal managers.

2.1. Field Site

Dawlish represents a beach-fronted vertical sea wall with a public walkway and critical railway infrastructure exposed to regular wave overtopping (Figure 1b). The railway line is the only rail connection to the SW of England. A section of the sea wall collapsed during extreme overtopping in February 2014. Due to the economic impact of the temporary loss (eight-week closure) of this railway line, the economic consequence of sea-level rise has been assessed [29]. However, detailed understanding of the spectrum of presentday overtopping drivers and how they may change the future frequency of overtopping has not been investigated other than with numerical approaches. Understanding the likely combinations of concurrent coastal interactions is critical for safe operation of the railway line, transporting both passengers and goods. The infrastructure owner, Network Rail, requires hazard forecasting days in advance to plan for the implementation of safety protocols: train specific speed limits, use of the landward track only, line closure, positioning of rolling stock to enable efficient timetable recovery and to minimise disruption to reduce delay and cancellation costs (e.g., Dawson et al. [29]). Regional speed limits are sometimes applied (often in response to gale force wind forecasts) causing impact over a greater area than necessary. An additional issue is that electric trains have their electronics positioned on the roof, as standard. After direct contact with salt water (potentially by a single wave) a train might not restart, although software updates now accommodate for multiple attempts enabling a train to recover while coasting, as long as the water drains away in time. Once a train stops in a station after travelling along a section of overtopping

track it can become stranded if it does not restart, blocking the line, as reported (https://www.bbc.co.uk/news/uk-england-devon-59559338, accessed on 1 February 2022) in the BBC news during Storm Barra. Reducing the speed limit if there is concern about the infrastructure (track/sea wall) potentially increases the vulnerability of the electric trains because they spend longer on the sea wall and are less likely to be able to coast their way out of a problem. Understanding the local frequency of overtopping, not only the discharge, is thus important for local hazard management.

Following collapse in 2014, a section of sea wall was rebuilt with a larger freeboard to mitigate overflow of the walkway. The railway line is located over 3.5 m landward of the sea wall crest behind a secondary wall (Figure 1b). During tides with forecast overtopping a response protocol is adopted. This is when flooding of the track could occur or damage to the sea wall, which could lead to undermining of the structure and wash-out of the track support, as happened in 2014. Operation protocols include having someone accompanying the train driver to monitor conditions and inspect the infrastructure for damage. The regional control centre is contacted for actions to be taken following the sighting of overtopping. The control centre use predicted high tide to assess if the hazard is likely to increase (incoming tide) or decrease (outgoing tide) based on the time of the call. Hazard predictions are not site-specific and without a wave overtopping frequency distribution relative to predicted high tide any local asymmetries in the hazard are unknown. In addition to daily operations, the South West Rail Resilience Programme is delivering phased upgrades to sections of the sea wall. Better understanding site-specific drivers of wave overtopping can support decision-makers by optimising when to change from maintenance to redesign for the monitored sections.

2.2. Monitoring

Instruments were deployed for a year (10 March 2021 to the 17 March 2022), during which overtopping (>23,000 individual waves at the sea wall crest) was recoded for 16% (112 tides) of the tides that year. Over this period the UK experienced six named storms (between 26 November 2021 and 21 February 2022), although due to the storm track positions only Atlantic storm 'Barra' caused overtopping (for 2 tides) out of those storms at Dawlish (7–8 December 2021). Most overtopping events were driven by typical conditions during the year. The months with most overtopping (i.e., on more than 10 tides) were April, May, October, December and March.

Individual wave overtopping events (plumes of wave spray travelling with horizontal trajectory over the sea wall structure) were counted using the WireWall capacitance wire system (validated in flume conditions [26]), ruggedised for long-term deployments [20]. WireWall recorded at 400 Hz for 6 h centred over every predicted high tide. Tidal predictions were obtained for Exmouth from the commercial POLTIPS-3 software [30]. Two WireWall systems were deployed over the cross-structure transect (Figure 1b) at the location where the sea wall collapsed in 2014 [31]. Both systems were programmed to run every high tide. The delayed mode data (downloaded from the logger and quality controlled [32]) are used to investigate the landward variation in wave overtopping frequency distributions. One system was installed on the seaward edge of the sea wall and the second system was installed on the seaward face of the secondary railway line wall. The two locations are referred to as sea wall crest (SC, using data from a wire 47 cm inland of the primary sea wall edge) and railway wall (RW, using data from a wire 3.3 m inland of the primary sea wall edge). The data represent the number of wave overtopping events reaching each wire position, i.e., travelling landward cross-structure.

No data loss occurred for SC, but power issues prevented data collection for RW from 03:00 (GMT) 3 October until 16:40 (GMT) 18 October 2021. No (quality controlled) wave

overtopping events reached the most inland wires on SC during these tides, suggesting no events would have been recorded further inland at RW. The WireWall data were processed to provide the timestamps of individual wave overtopping events. Camera footage indicates overtopping at this site occurs as vertical plumes of spray. Quality control (QC) is applied to each wave event detected. The WireWall system uses pairs of capacitance and copper wires to measure the rate of discharge of each capacitance wire when a wave bridges the (1 cm) gap between the pair. QC first checks that the capacitance discharge signal caused by an individual overtopping wave exceeds the dry baseline capacitance value of that wire pair, which is calculated every 10 min. This isolates the wave events. The second check is that another wire pair adjacent to or seaward of the wire pair of interest registers the same event, i.e., detects an event within 2 s. The second check removes isolated splashes or human/animal interference. The open scaffolding framework of the WireWall systems was designed to ensure the wires were exposed to overtopping from all directions, with no directional sheltering from existing infrastructure. The 1 cm gap between the wires in the pair prevents rain creating false overtopping events but allows overtopping spray droplets of at least 1 cm diameter or jets of water to be detected.

An anemometer was installed at approximately 9.4 m *OD* height (~4 m above the sea wall) adjacent to the WireWall system (SC) on the sea wall crest (Figure 1b). The height was limited by safety requirements for the equipment to be able to fall seaward of the railway line wall so may be influenced by surface friction but provides a good indication of the wind conditions. The nearest available wind data from long-term monitoring were West Bay Harbour (50°42.640′ N 2°45.837′ W), on the other side of the bay to Dawlish, or Channel Lightship 62103 (49°54′ N 2°54′ W), which is offshore, thus potentially neither are representative of the local wind conditions influencing the overtopping spray. Wind data were recorded 4 August 2021 to 24 November 2021 and 6 January 2022 to 3 May 2022 and were processed to provide wind speeds and directions at 10 min intervals. Given approximately 6 months of data are missing 10 min data from West Bay are also provided in Appendix A to compare with Figures 2e and 3g,h.

Alongside the bespoke local WireWall and Anemometer instrument deployment, long-term wave and water level measurements (Figure 2) are available from the National Network of Regional Coastal Monitoring Programmes (NNRCMP) of England (located in Figure 1a). For the deployment period the quality-controlled measurements were obtained to limit data loss, remove erroneous data and obtain advanced statistics (e.g., the wave energy period introduced to monitor coastal overtopping hazard from swell wave contributions along the south coast of England, ref. [33]). The data used were from the Exmouth station 117 (water levels recorded at 10 min intervals, approximately 4.5 km alongshore) and the Dawlish station 103 (wave conditions recorded at 30 min intervals, approximately 3 km offshore). These observed waves and water levels were input at the seaward boundary of a measured beach profile to obtain the predicted wave height at the structure toe (Figure 2f). The wave transformation was calculated using the Janssen and Battjes [34] parametric surf zone model with a toe mound factored into the calculations following Stokes et al. [15] to match the numerical predictions in the existing forecast service (OWWL) available to coastal managers across the SW region as a public NNRCMP resource. The profile from the upper beach to the wave buoy was compiled from the most recent bathymetry survey (2020, from the SW coastal monitoring programme) and a laser scan of the upper beach (collected February 2022 during instrument deployment).

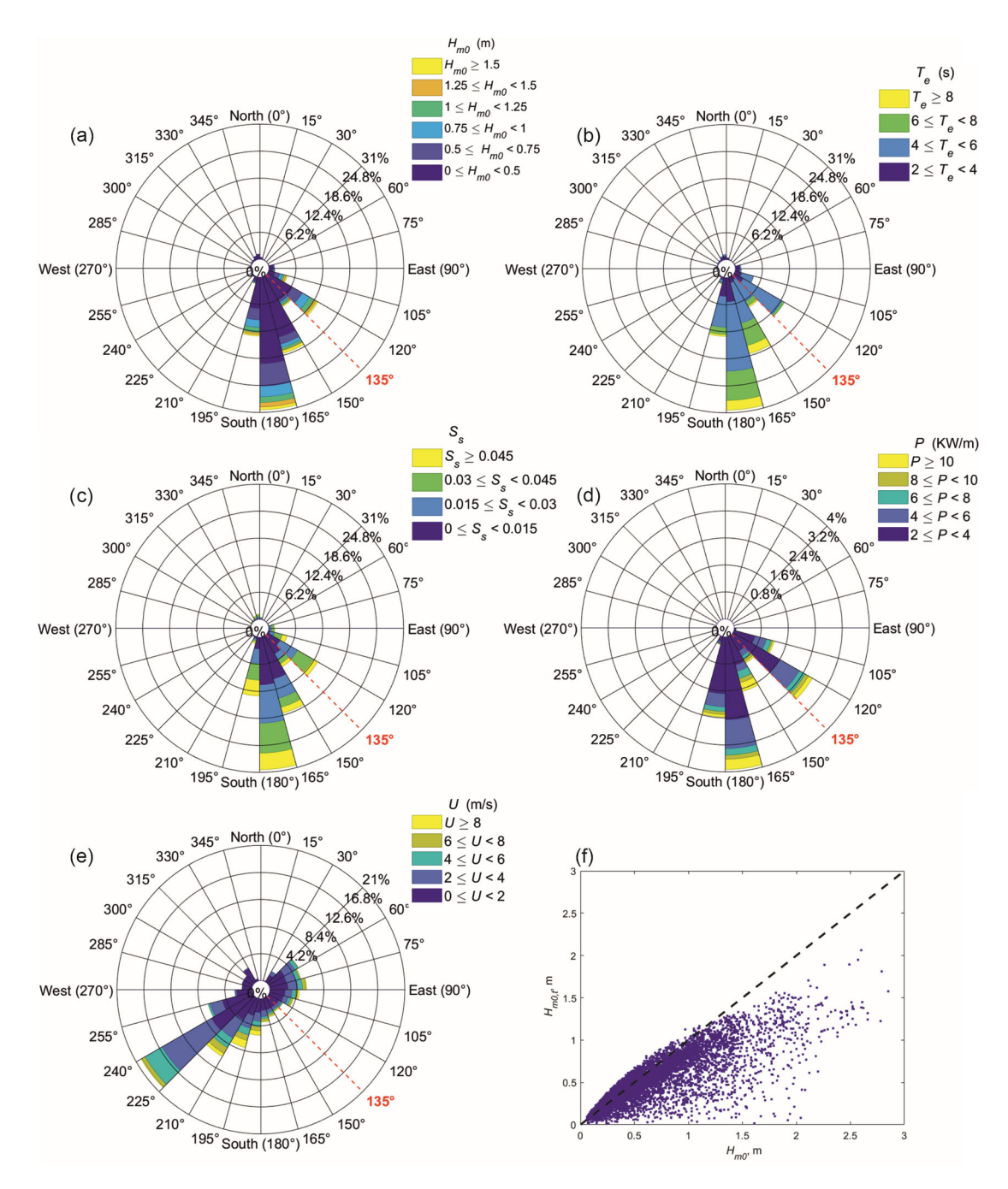


Figure 2. The observed wave–wind climate in Dawlish, directional roses (made with code from Pereira [35]) of (**a**) zero moment wave height, H_{m0} , (m) measured at the wave buoy, (**b**) wave energy period, T_e , (s) measured at the wave buoy, (**c**) wave steepness, S_s , measured at the wave buoy, (**d**) wave power, P, (KW/m) measured at the wave buoy, (**e**) wind speed, U, (m/s) measured at the WireWall deployment location and a scatter plot to show (**f**) the predicted wave height transformations at the sea wall toe, $H_{m0,t}$ (m), from those measured at the buoy, H_{m0} (m). The onshore bearing is at an angle of 135°, highlighted in red with a red dashed line.

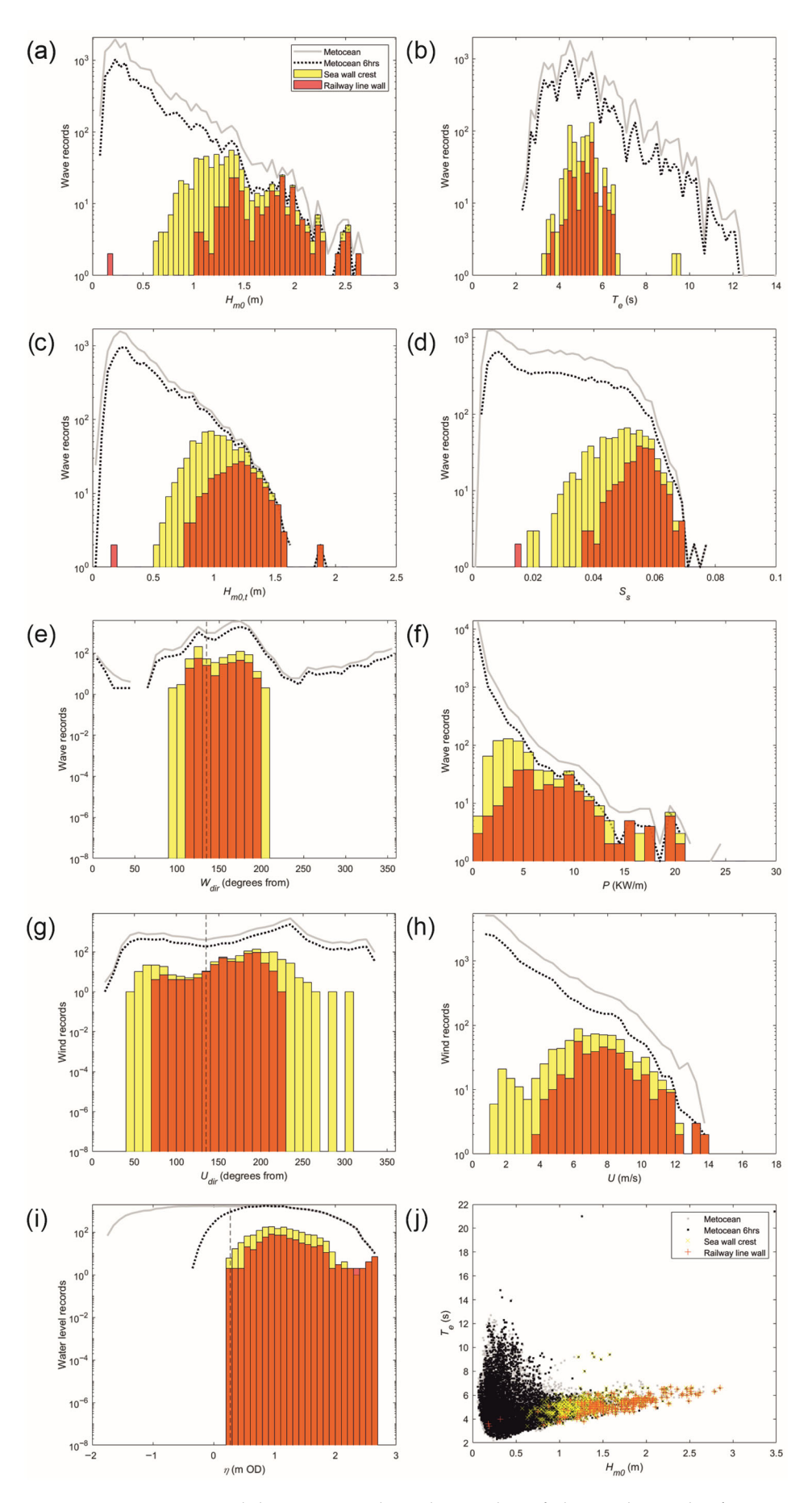


Figure 3. Histograms with log-y axis to show the number of observed records of metocean (MO) conditions (grey line) and those conditions associated with wave overtopping at the sea wall crest

(SC; yellow bars) and railway line wall (RW; orange bars). The metocean data are near-continuous for the year (grey line) but the conditions compared with overtopping are limited to the 6 h high tide WireWall measurement window for every tide during the 1-year period (black dashed line). (a) Wave height, H_{m0} , (m) measured at the wave buoy. (b) Wave energy period, T_e , (s) measured at the wave buoy. (c) Transformed wave height at the structure toe, $H_{m0,t}$, (m). (d) Wave steepness, S_s , measured at the wave buoy. (e) Wave direction, W_{dir} , (degrees) measured at the wave buoy with the vertical dashed line indicating the onshore direction. (f) Wave power, P, (KW/m) measured at the wave buoy. (g) Wind direction, U_{dir} , (degrees) with the vertical dashed line indicating the onshore direction. (h) Wind speed, U, (m/s). (i) Water level, η , (m OD) with the vertical dashed line indicating the mean water level over the 1-year period. A scatter plot (j) of observed H_{m0} against T_e colour coded if wave overtopping occurs at SC or RW. Wave observations were available at 30 min intervals, while water level and wind observations were available at 10 min intervals.

The coastal metocean data provide information about the spectrum of conditions during the year at Dawlish. The largest range in wave heights (Figure 2a) and wave energy periods (Figure 2b) are from the SSE, both with the smallest and largest conditions being observed from this direction. The SSE waves represent low (<0.5 m) swell waves to large wind seas (see Figure 3j). Waves from the SE represent (short period) wind waves. While the highest waves are from SSE (<3.5 m), waves from both the SE (<2.2 m) and the SSE often reach 1.5 m. A higher proportion of the SE waves are steeper than 0.03 (Figure 2c), while from the SSE waves with low steepness occur relatively often. The highest power waves occur from SSE (Figure 2d), however, a large proportion of the waves from all directions are low power (<4 KW/m). The winds are rarely directly onshore (135°) at the sea wall (Figure 2e and Appendix A Figure A1b) and waves within the bay from SSE and SE have a similar low likelihood of having a following wind. Comparing the coastal wave and transformed wave heights, it is seen (Figure 2f) that depth limitation can become more influential for wave heights > 1 m. For the largest waves to maintain their height they must coincide with higher tidal elevations. The occasional very large steep wind waves from the SSE are thus more likely to be depth-limited than the moderately large steep wind waves which are more common from the SE than SSE.

The timestamp of the individual wave overtopping events is compared with the time of the metocean data or the time of predicted high tide to produce a set of frequency distributions (Section 3). Data from the National Monitoring Networks represent a nearcontinuous record, providing a year of coastal conditions. To enable comparison of the (driving) metocean conditions with the (resultant) occurrence of individual wave overtopping events (Section 3.1), each metocean record is assigned a flag to indicate if wave overtopping occurred at either SC or RW within the monitoring interval of the metocean record. For example, wave height data are provided at 30 min intervals. If overtopping at SC is recorded within 15 min before to 15 min after the wave data timestamp that wave condition is flagged as overtopping at SC. Any data loss in the metocean monitoring impacts both data sources equally. For metocean data outside the 6 h WireWall monitoring period there will be no information thus no overtopping recorded. Occasionally, during high-energy conditions, wave overtopping had started before or continued after the time the WireWalls turned on/off, but the number of overtopping waves is likely to be low during the lower tidal elevations. When considering the wave overtopping hazard relative to the time of predicted high tide (Section 3.2), all individual wave overtopping events are included within the histograms.

To associate each individual wave overtopping event to a transformed wave height (Section 3), the transformed waves were linearly interpolated to the time of overtopping. If there were no transformed wave data (due to no coastal monitoring input) up to an hour before or after an overtopping event, the nearest wave height condition is assigned.

If there are no transformed wave data for over 1 h either side of an overtopping event, no transformed wave information is assigned to that event. Uncertainty in the wave transformation will occur due to the static nature of the beach profile, no inclusion of wave–structure or wave–current interactions, and no inclusion of swash or wave setup, all of which potentially modify the water depth and wave conditions at the toe. The transformed wave conditions are obtained at approximately 5 m seaward of the vertical sea wall, which at the time of the beach scan was at an elevation of -0.62 m OD.

2.3. Limitations

WireWall and the local anemometer were deployed for a year to complement existing monitoring networks and forecasting services established for coastal management. These data provide information about the concurrent environmental conditions that most frequently cause wave overtopping but do not capture process interactions over a cross-shore transect from nearshore to land. Application of the 1D numerical (OWWL) predictions provides insights about the wave transformations using previously established code, which has been validated to become a trusted resource for regional hazard management and now rarely undergoes update. Ideally a laser scanner able to measure the beach level at low tide and wave and water levels at the structure toe during high tide would have provided more detailed data. However, laser instruments are power hungry when run at the required sampling frequencies and with no mains power supply maintenance costs would have escalate to collect the year-long dataset (further complicated by this deployment taking place during the COVID-19 national lockdowns).

The WireWall data are constrained to 6 h measurement windows centred over high tide. Analysis of the measurements show minimal data were lost due to this constraint, applied to conserve batteries to support a 3-month maintenance cycle. The 6 h window was considered appropriate by local coastal practitioners to capture conditions. Even with this limitation continuous 6-hourly data are obtained to compare with available monitoring of the driving conditions (provided at 10 or 30 min intervals). Traditionally physical and numerical experiments focus on discrete combinations of wave-water level conditions, often focusing on extremes, missing the detailed time-variability during the different tide-weather events, especially of low energy high probability events. While numerical simulations can efficiently cover longer timescales, they require validation/calibration for a wide range of site-specific conditions and studies often focus on historic storm impacts or extreme (high energy low probability) scenarios for scheme design/assessment.

The wave overtopping data are limited to providing information on the number of overtopping waves due to uncertainty in the measurement of the depth of the overtopping event (plume) and more importantly the inability to measure the horizontal velocity component during large overtopping events due to the spacing between the wire pairs within the WireWall system (which on average was approximately 40 cm). The spacing was not wide enough to distinguish different start times of the overtopping events through the WireWall rig due to overtopping water falling onto all wires simultaneously. This was the first deployment of the WireWall system in a remote high energy location in a stand-alone configuration (no personnel on site) for long-term monitoring to access the capability of the technology development. While the design was rugged for a 1-year deployment the PTFE coating of the capacitance wire was not as self-cleaning as expected influencing the depth measurement. The wire pair spacing can be adjusted but was restricted to allow for space between the two WireWall systems to allow for the 2 m COVID-19 social distancing requirement in public places during the deployment. Further materials tests are required in future research and ambitions have been established to wirelessly synchronise multiple small WireWall systems to measure speed across larger distances (>2 m) with minimal

intrusion across access routes. The desire is to monitor wave overtopping speeds and discharge long term. Capturing data on the high probability low intensity overtopping events will improve coupled wave–tide–surge-overtopping models. While these models capture the interactive processes and there is confidence in overtopping predictions for extreme events, coastal infrastructure managers now also require certainty in predicting the more regularly occurring overtopping events.

3. Results

All available metocean and overtopping observations are analysed to assess the key overtopping drivers and their thresholds during the year. The new understanding and trigger levels are used to explain the time-evolution of a single event, Storm Barra (7–8 December 2021).

3.1. Wave Overtopping Drivers

Figure 3 illustrates the frequency distribution for different coastal metocean conditions (in grey), including Storm Barra, recorded by existing monitoring networks for the year of interest. A subset of these metocean conditions that were recorded during the 6 h periods centred over every predicted high tide (i.e., when the WireWall systems were also running) during the 1-year period is provided (in black), isolating the coastal conditions associated with measured overtopping (histogram bars). When a metocean record coincides with overtopping at either the sea wall crest (SC; in yellow) or railway line wall (RW; in orange), that record contributes to the respective overtopping frequency distribution (bar) and can be directly compared with the high tide frequency distribution of the parameter in question (in black). Comparison of the 6 h high tide conditions (in black) and the continuous conditions (in grey) over the year, show that only the water level range (Figure 3i) is limited while most wave and wind conditions coincide with high tide during the year. Parameters which vary most in response to the tides are the transformed wave height at the structure toe (Figure 3c) and wave steepness at the wave buoy (Figure 3d). The convergences of the data (black and grey lines) for higher values in these parameters, highlight steeper coastal waves and higher waves at the structure toe are likely to occur around high tide. It should be noted that the log-y scale of Figure 3g noticeably flattens the directional distribution, smoothing the large dominance in wind direction from the SW (Figure 2e).

For overtopping to occur at Dawlish, the coastal waves (Figure 3a) need to be of moderate size ($H_{m0} > 0.65$ m), especially for overtopping to travel a distance landward ($H_{m0} > 1.0$ m). Large wave conditions ($H_{m0} > 1.5$ m) have a low probability of occurrence (Figure 2a) limiting their coincidence with high tide (± 3 h). When they are coincident with high tide elevations (Figure 3a), they often cause overtopping as the depth limitation of these waves (Figure 2f) is reduced. The transformed wave heights, $H_{m0,t}$, reaching the structure toe (Figure 3c) need to exceed 0.5 m to cause overtopping of SC and 0.75 m to travel landward to RW. The waves that overtop are steep wind waves (Figure 3d) with a (typical and) relatively low energy period (Figure 3b) but represent the full range of wave powers (Figure 3f).

Overtopping is most likely for a restricted range of SE directed waves $(110^\circ-140^\circ)$ and for a wider range of direction from SSE waves $(150^\circ-190^\circ)$ (Figure 3e). These directions align to the directions with most waves (Figure 2a, primary wave direction SSE: $150^\circ-180^\circ$ and secondary direction SE: $120^\circ-135^\circ$). SE waves $(125^\circ$, Figure 3e) have the greatest likelihood of overtopping, especially at SC. Compared with SSE waves SE waves are often associated with a low energy period (Figure 2b). A large proportion of the SE waves are of moderate size (Figure 2a) and steepness (Figure 2c), making them less likely to be depth-limited, while the waves from SSE can range from small swell waves to large wind

waves (Figure 2a,b). This slightly increases the likelihood of SE waves overtopping (at SC) although SSE waves are more common. Larger waves ($H_{m0} > 1$ m) that cause overtopping to reach RW have a lower probability of occurrence from both directions (Figure 2a) and are likely to be depth-limited, unless coincidental with high tide, minimising a directional bias in maximum frequency. The waves are less likely to reach RW when there is a greater E component in the wave direction (Figure 3e). This is probably due to large waves being associated more frequently with the SSE direction (Figure 2a).

Overtopping is more likely to occur with strong onshore winds [11], which are rare (Figure 2e and Appendix A Figure A1b). The topography of the bay (headlands and cliffs close to the site of interest) has a noticeable influence on the wind directions. The SC overtopping frequency distribution follows that of the wind direction (Figure 3g). Suggesting that the wave momentum is a main driver for inland transport of the overtopping rather than the wind. For the overtopping to reach RW the directional range for which overtopping occurs is more limited to wind directions with an onshore (or alongshore) component (70°–230°). While overtopping can occur under most wind speeds, it is most likely when winds are 4–12 m/s and the winds need to exceed 3.5 m/s for overtopping to reach the RW (Figure 3h). The strongest winds have a lower likelihood of coinciding with high tide, limiting coincidental overtopping occurrences, but when they do coincide overtopping is likely.

For overtopping to occur, water levels need to just reach or exceed the mean water level (0.27 m *OD*, Figure 3i). Storm events (e.g., Barra, Section 3.2) can have significant impact at the highest water levels, but when removed it is rare for overtopping to occur for the highest water levels (>2 m *OD*) due to the low statistical probability of the spring high tide coinciding with energetic wave conditions. During the deployment the highest and lowest predicted high tides were 2.31 m *OD* and 0.44 m *OD*, respectively. Generally higher water levels are required to enable larger waves to cause overtopping to travel further landward.

For Dawlish, wind seas dominate the wave climate, especially from the SE, and are associated with overtopping (T_e < 7 s; Figure 3j). The larger and steeper the wind waves, the more likely the overtopping is to be transported landward. While higher tidal levels enable these conditions to reach the sea wall, the probability of large steep waves and (strong onshore) winds occurring at high tide, let alone the highest tides, is limited.

In Figure 4 the time of every individual wave overtopping event at SC (Figure 4a) and RW (Figure 4b) is plotted relative to predicted high tide. When the total number of wave overtopping events are separated into transformed wave height categories we see the following:

- 1. Small waves ($H_{m0,t}$ < 1 m) have most impact at the onset/outset of the rising/falling tide, but low impact for c. 90 min either side of predicted high tide. These waves are most likely to represent small coastal waves and depth-limited coastal waves (Figure 2f) impacting the sea wall. The high tide reduction in the number of wave overtopping events is most likely due to reflection as seen in the video footage, e.g., 8 March 2022 [36].
- 2. Moderate-size waves ($H_{m0,t} = 1-1.5$ m) contribute the most to overtopping during the 6 h monitoring period and are likely to be depth-limited waves (Figure 2f). A reduction in the number of overtopping events occurs roughly an hour either side of predicted high tide and the smaller waves within this category are also likely to experience (partial-)reflection at this time.
- 3. Large waves ($H_{m0,t} > 1.5$ m) overtop for a limited duration. They can overtop at high tide (for ~2 h) when depth limitations on the waves are reduced or when a storm passes if the elevated water depths (by surge and wave setup) are sufficient to

maintain the wave heights reaching the structure toe. In this distribution Storm Barra causes noticeable overtopping from ~90 min after predicted high tide (see Section 3.2), significantly contributing to the high energy categories of the frequency distributions.

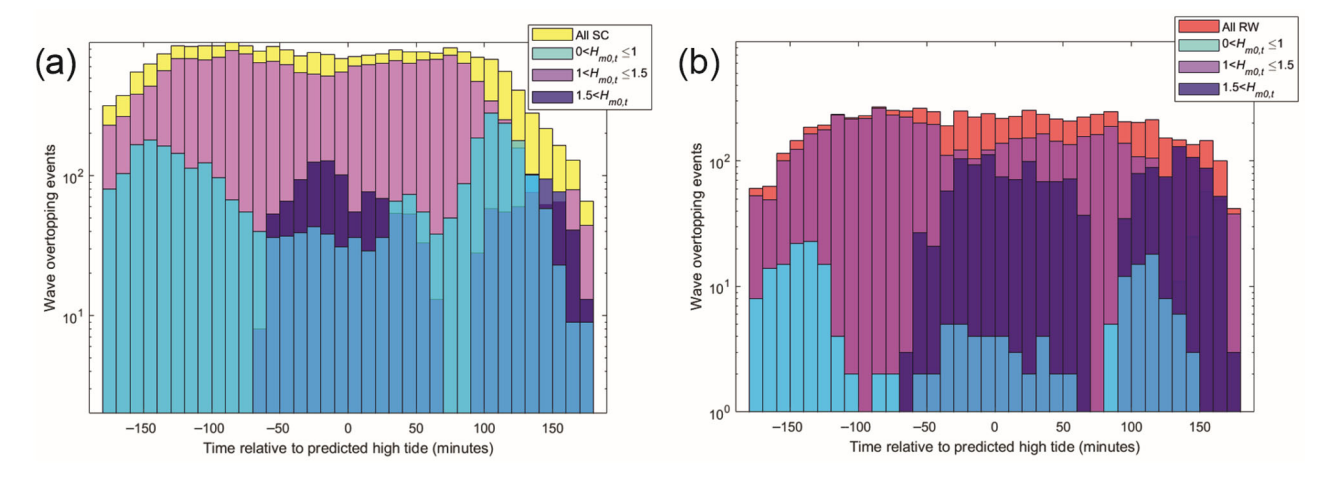


Figure 4. Histograms with log-y axis of wave overtopping events measured by the WireWalls from 3 h before to 3 h after predicted high tide (0 min) for 1 year separated into transformed wave height categories, $H_{m0,t}$ (m). Data from (a) the sea wall crest (SC; in yellow) and (b) the railway line wall (RW; in orange). 'All' data are measured by the WireWalls, and the ' $H_{m0,t}$ ' wave transformation categories are calculated from the wave buoy and tide gauge monitoring over the same time intervals. Gaps in the coastal monitoring prevent all wave overtopping events being categorised and the bar transparency creates some differences in shading to that in the legend where data overlay.

The slight asymmetry in the wave overtopping frequency distribution at SC (a higher peak on the rising tide and rapid reduction on the falling tide after 100 min) could be the result of tidal (elevation) asymmetry. However, wave–current interaction is likely to be important at this site in influencing the wave dynamics for all or certain wave directions. Tidal predictions indicate slack tide is prior to predicted high tide (~1 h), thus, most of the overtopping measurement window experiences an ebb flow (increasing for ~2 h after predicted high tide).

3.2. Storm Response, Barra

Storm Barra impacted two tides on the 7 and 8 December 2021. We assess the temporal variability in coastal conditions (Figure 5) compared with the thresholds for overtopping in Figure 3. No wind data were recorded during this period, either at the WireWall location or West Bay, the nearby secondary data source; we therefore focus on the wave and water level conditions.

First tide: The (southerly) coastal waves increased in size as the tide rose (Figure 5a,b). Overtopping had started when the WireWall systems turned on (06:00 (GMT), SC, Figure 5c) and the number of overtopping events increased, reaching the railway line wall later, an hour after the systems turned on (07:00 (GMT), RW, Figure 5d). The waves were not particularly depth-limited during the rising tide, and a relatively large-sized transformed height was maintained during the rising tide. At SC, the number of overtopping waves follows the increase in the coastal wave height. At RW the overtopping starts later, when the transformed waves are larger, and the number of overtopping events rapidly plateaus. After high tide, the coastal waves continue to grow, but the falling tide impacts the (steep) waves by causing depth limitation. There was a sudden drop in overtopping events (in the last 30 min of the high tide measurement window) in response to the drop in transformed wave heights (roughly in agreement with Figure 4 as the representative distribution switches from $1 \text{ m} < H_{m0,t} \le 1.5 \text{ m}$ to $H_{m0,t} \le 1 \text{ m}$). This was preceded by a drop in coastal wave height,

suggesting a change in the wind conditions occurred, immediately reducing the transport of the overtopping events landward while there was a lag in wave decay. Without local wind data this cannot be confirmed. However, the camera overlooking the WireWall shows a reduction in the transport of spray inland soon after 11:30 (GMT). Before 11:30 (GMT) wind is clearly influencing the inland transport of spray for the vertical overtopping events. After 11:40 (GMT) the wind transport inland is minimal. The transformed significant wave height during overtopping (Figure 5b) exceeded 1 m, which is above the wave threshold for overtopping (Figure 3c). Water levels of 0.2 m *OD* occurred (Figure 5a) close to the time the WireWall system turned on/off, enabling overtopping (Figure 3i).

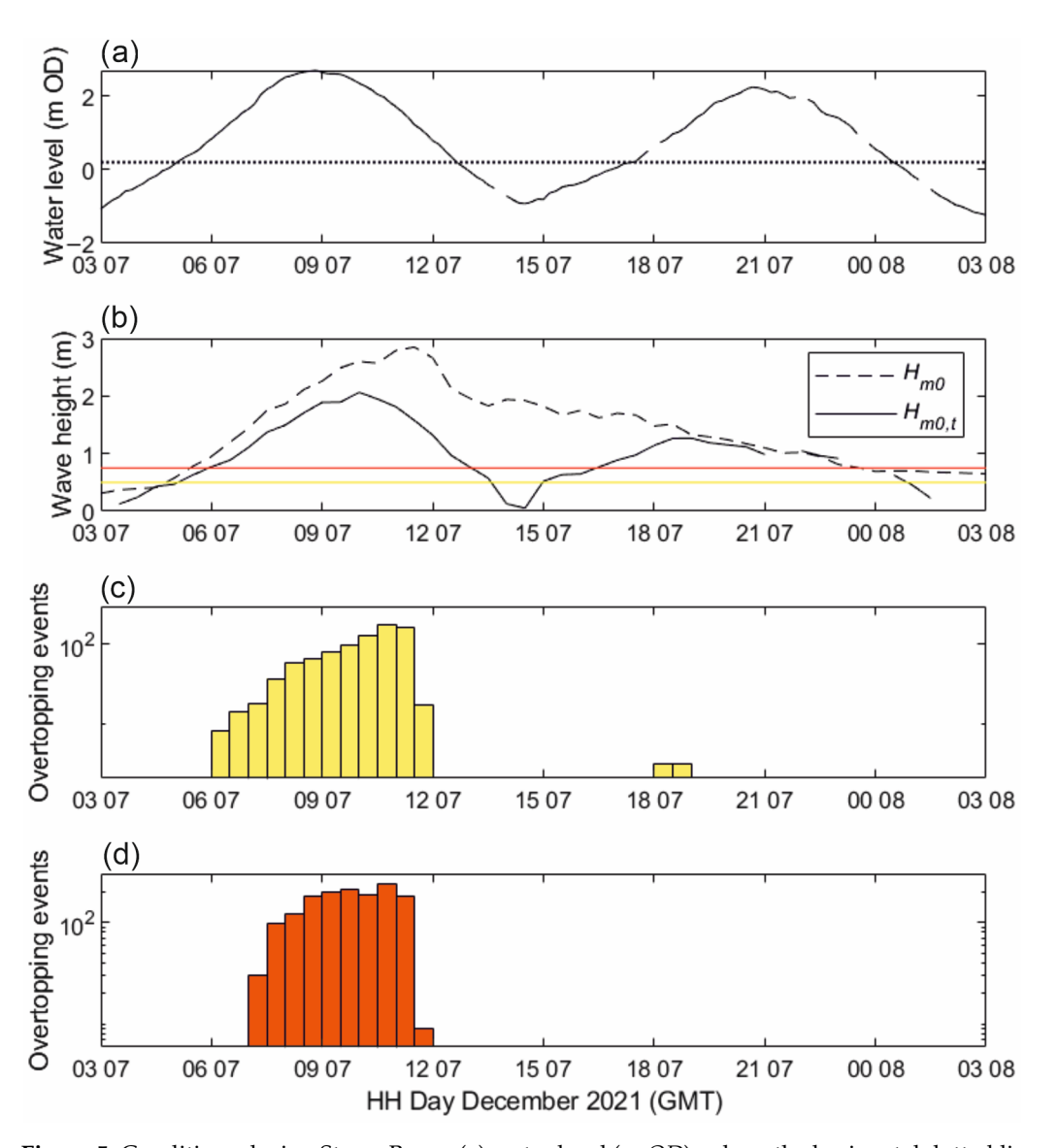


Figure 5. Conditions during Storm Barra: (a) water level (m OD), where the horizontal dotted line is the threshold for overtopping (Figure 3i, 0.2 m), (b) coastal, H_{m0} , and transformed, $H_{m0,t}$, wave height (m), where the solid horizontal lines are the thresholds for overtopping for the transformed waves (Figure 3c), colour coded by the location of the overtopping (SC in yellow, 0.5 m, and RW in orange, 0.75 m), (c) number of wave overtopping events at the sea wall crest (SC) and (d) number of wave overtopping events at the sea wall crest (RW).

Second tide: The coastal waves waned (Figure 5b) and were still noticeably depth-limited on the rising tide. Some overtopping occurred at SC (Figure 5c) once the water level threshold (Figure 5a) was exceeded. No overtopping reached RW (Figure 5d) although the wave thresholds are exceeded, suggesting that the wind is not transporting the vertical

wave plumes inshore and/or the return lip on the structure is able to deflect much of the uprush offshore. Without local wind data this cannot be confirmed. The camera was operational until just before 17:00 (GMT) due to limited daylight. Footage of the spray alongshore from the WireWall system, generated by wave impact on beach access steps on the sea wall, was not being blown inshore but being deflected offshore. Depth-limitation ceases at high tide and overtopping stops, suggesting that the transformed waves with $H_{m0,t} > 1$ m (once the water level > 0.2 m OD) are reflected (by the vertical wall or return lip) during this, relatively high, high tide (as suggested in Figure 4a).

4. Discussion

This paper focusses on the wave overtopping event frequency distribution for 1-year of data, not the magnitude (discharge or volume) of overtopping, to understand the most likely metocean drivers that cause overtopping at Dawlish. Identifying the variation in most likely times of overtopping occurrence relative to predicted high tide at different cross-structure locations illustrates the complexity of hazard communication for different infrastructure users, e.g., in this case the public amenity and railway network. We explore a full spectrum of conditions rather than storm events only. It is well known that coastal wave heights are modulated by (1) the tide through water level and current interactions influencing: refraction, steepening, dissipation, bottom friction, reflection; and also modified by (2) interactions with shallow morphology and sea breezes [37]. Having a frequency distribution of overtopping events alongside that of the metocean monitoring parameters can optimise site-specific safety procedures and protocols, although every weather system will create its own event-scale frequency distribution due to the timing of the wave propagation relative to the tide.

For Dawlish, wind waves dominate the wave climate and are the main contributor to wave overtopping, not long-period low-height swells due to the large (>~3 m) freeboard. The larger wind waves are able to travel further landward across the structure when they overtop. The transformed wave height at the structure toe is critical in enabling overtopping, as depth limitation is a key factor in how overtopping is modulated through the combination of offshore wave height and tidal level. Moderate-sized waves ($H_{m0} = 1-1.5$ m) that occur most frequently through the year are the biggest contributors to overtopping as they do not require the highest (low probability spring/storm) tidal levels to maintain a significant height on impact with the sea wall. These waves are common from the SE at Dawlish, while waves from the SSE cover a wider spectrum of conditions and are the dominant wave direction.

For vertical sea walls with a large freeboard relative to the tide, wave reflection at high tide can limit or even stop the occurrence of overtopping if the water is deep enough relative to the incident wave. Given the spectrum of wave heights within a wind sea, the frequency of wave overtopping is likely to change in response to the tidal elevation depending on the coincidental wave conditions. A reduction in the number of overtopping waves at high tide for Dawlish can be observed and so can reflection of some of the waves within the spectrum. At this time, the run up of the waves does not always exceed the freeboard or is returned by the lip as it is much less explosive. The wave overtopping can be analysed using the transformed wave height categories. Small-sized waves ($H_{m0,t} < 1.0 \text{ m}$) have the longest duration of reduced overtopping at high tide because the waves are likely to reflect under more of the high tide conditions. Some moderate-sized waves ($H_{m0,t} = 1.0$ –1.5 m) can also reflect close to high tide, probably on the higher neap and spring condition, and the maximum overtopping is most likely to occur approximately 100 min either side of high tide at Dawlish. There is a slight rising tide dominance in the number of overtopping events for moderate-sized waves, which creates a slight overall asymmetry in the overtopping event

frequency distribution for the year. Large-sized waves ($H_{m0,t} > 1.5$ m) only overtop for a limited duration around high tide (~1 h before and after unless there is a surge contribution to the water levels) and contribute least to the overtopping event frequency distribution. This is because at lower tide levels the larger waves will break on the beach further away from the sea wall. Thompson et al. [38] also found that storm-driven overtopping of a vertical sea wall occurred an hour before and after high tide with a high frequency of events occurring at high tide. Further inland (at the railway line wall) the wave overtopping event frequency distribution is much more constant around high tide because only overtopping of the largest moderate-sized and large-sized waves travels landwards and these waves are less likely to reflect.

Sea-level rise, beach lowering and/or a change in the wave climate could modify the present-day overtopping event frequency distributions. Research into storm driven overtopping has found the influence of the subtidal beach profile can have a varying role in influencing the overtopping of different intensity storms [19]. Stein and Siegle [39] found that a wider and flatter beach profile fronting a sea wall provides greater protection. Stokes et al. [15] found overtopping hazard increases for storms during lower beach volumes. Storm-driven scour at a structure toe can also change the water depth and increase the overtopping discharge of an individual storm, although the size of the increase will vary depending on the storm's position within a sequence of events [40]. Many overtopping studies are laboratory-based with limited resources to explore numerous water level—wave combinations, often creating a focus on storm wave impact rather than tidal influence on the vast range of more typical wave conditions. Numerical investigation into tide-surge influence during a storm peak by Xie et al. [41] found overtopping discharge increased, due to larger wave heights at the structure toe. When they considered sea-level rise the overtopping discharge increased further. Raising the sea wall by an amount equivalent to the sea-level rise scenario did not completely mitigate the increase in overtopping. Assessment of overtopping discharge at vertical sea walls across England under rising sea level scenarios up to 1 m found a non-linear response to return period, ranging from over a factor of 4 increase for 1 in 1-year events to over a factor of 12 increase for 1 in 1000-year events [14]. However, the study does not explore how the overtopping event frequency distribution over the tidal cycle could change influencing the annual duration of overtopping and/or the annual number of waves overtopping. Both these quantities are critical for infrastructure operators, particularly in transport, to build coastal resilience. Here, we find many overtopping waves within the 1-year frequency distribution are below the 0.25-year return period, defined as the storm threshold by the National Network of Regional Coastal Monitoring Programmes of England and is presently calculated to be $H_{m0} = 2.63$ m or $T_e = 11.20$ s at the Dawlish wave buoy. Figure 3a,b show nearly all of the overtopping events at Dawlish are caused by wave conditions below these storm thresholds. The ability to predict future overtopping is critical to assess future disruption to the railway line at Dawlish. Using historic events to project sea level impacts found the number of days with railway line restrictions could increase to 84–120 days a year by 2100 depending on the sea-level rise scenario applied [29]. Without understanding how tidal interactions and waves across the full spectrum will respond to deeper water introduces uncertainty in this projection, which is focused on daily incidents, because understanding the wave-by-wave overtopping hazard is critical given that a single wave could damage a train.

The annual duration of wave overtopping at any vertical sea wall will be the sum of the different contributions from the full wave spectrum. How the individual wave contributions change in future will vary due to local wave–tide–morphology interaction. Deeper water levels in front of a sea wall due to sea-level rise and beach lowering will cause complex and non-linear changes in the yearly overtopping event frequency distribution.

Figure 6 is a schematic suggesting plausible changes in the yearly wave overtopping event frequency distribution for Dawlish, as an example of a beach fronted vertical sea wall exposed to a large spectrum of wind sea conditions. The present-day overtopping event frequency distribution for vertical sea walls is likely to have a common shape, i.e., the sum of a dominant 'M-shaped' moderate-sized wave distribution (Figure 6a) and smaller 'n-shaped' large-sized wave distribution (Figure 6b). Deeper water at the toe of a vertical sea wall will cause a longer overall duration of when wave overtopping could potentially occur either side of high tide (Section A, Figure 6) for both moderate- and large-sized waves. However, the number of waves overtopping within this extended duration will depend on the wave size. An increased duration may not simply enable time for more waves to overtop. For commonly researched large-sized (storm) waves, the number of waves overtopping for a limited number of hours at high tide is likely to increase (Section B, Figure 6b) as depth limitations reduce. Overall, both the number of large-sized waves overtopping at any instance and the duration of large-sized wave overtopping is likely to increase (Figure 6b). This in agreement with the findings of, for example, Hames et al. [14] and Almar et al. [9]. It should be noted there is the chance some of the waves at the lower end of this category could start to reflect at high tide. The rarely researched response of moderate-sized waves (<1.5 m, i.e., below the storm threshold) is much more complex, but crucial to understand the annual overtopping hazard due to their dominance within the yearly event frequency distribution. Overall, the duration of when moderate-sized waves could overtop will extend, but the overall number of waves overtopping could increase or decrease (Figure 6a). It is hypothesised the total number of waves will potentially decrease. At high tide (section B Figure 6a) wave reflection could occur for a longer duration and potentially occur for more waves within the moderate category, both reducing the overtopping frequency for a few hours over high tide. If the largest waves in this category experience reduce depth limitation, they are more likely to move into the large wave category and contribute further to the increase in large-sized wave overtopping at high tide. The water level enabling a maxima in the number of waves overtopping (sections C Figure 6a) will occur earlier and later in the tide, which is when the water levels change more quickly, potentially reducing the duration of maximum overtopping frequency. Thus, the number of waves overtopping is again likely to reduce.

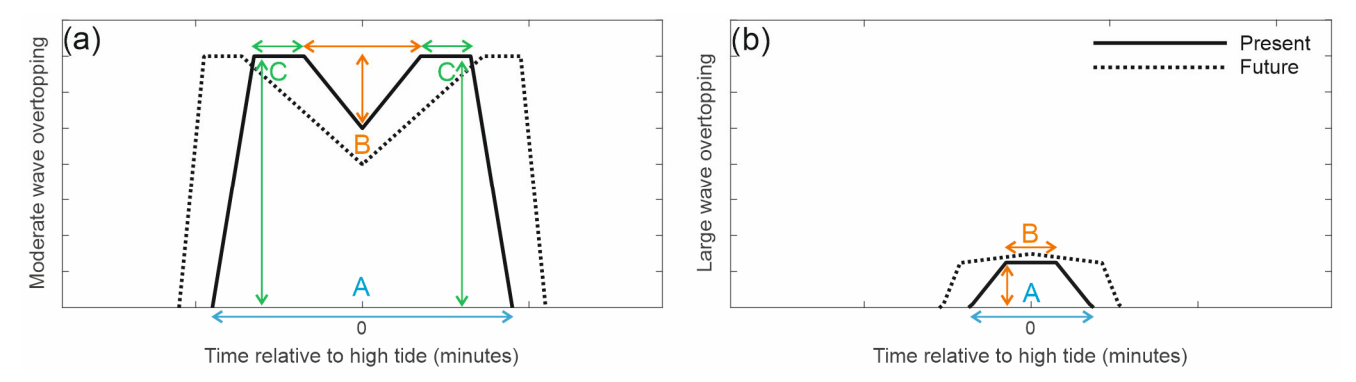


Figure 6. Schematic of the present-day (solid line) and proposed future (dashed line) wave overtopping event frequency distributions for (a) moderate-sized waves at the structure toe and (b) large-sized waves at the structure toe. The proposed future distribution is for deeper water levels due to sea-level rise and/or beach lowering.

While there is confidence that the duration for which overtopping can occur during a tide, and thus year, will increase with sea-level rise, the change in the total number of waves overtopping during this time is less clear. It is speculated that at the crest of a sea wall the total number could go down, as moderate-sized wave events are more common than

large-sized wave events. However, the number of overtopping waves travelling further landward is likely to increase in occurrence as this is controlled by the large-sized waves. Large-sized waves are associated with higher discharge, which is why research focused on storm events finds an increase in flood hazard. For moderate-sized waves the change in flood hazard is rarely studied and will be a complex balance between the overall number of lower discharge waves overtopping and their frequency, which could impact the built-in drainage capability within a sea wall structure.

Future changes in the local wave climate may also impact the wave transformation processes and change the dominant wave direction, size and frequency, causing overtopping. Water depths are likely to mediate changes in the magnitude and frequency of the occurrence of overtopping through wave—tide interactions. More frequent moderate-sized waves could simply increase the number of events within the event frequency distribution exaggerating the M-shape (Figure 6a) due to a balance between reflecting and depth-limited processes, while more frequent large-sized waves will be depth-limited unless water depths increase by a required amount. The resulting overtopping event frequency distribution will again be a balance in the overtopping due to different size wave conditions and the depth-limited verses reflective conditions. A shift in prevailing weather tracks is unlikely to change the swell wave contribution at Dawlish due to the limited local fetches, but could change the wave direction most often associated with wave overtopping in response to a change in the height of the wind sea conditions. The direction with most frequent moderate wind seas is most likely to cause overtopping and the direction with the largest waves most likely to cause overtopping that travels landward.

Understanding the metocean drivers that cause most of the present-day wave overtopping, provides useful information to support future planning. Assessing the potential change in the overtopping frequency distribution suggests that the number of waves overtopping the sea wall crest could reduce in a year but more of those overtopping waves will travel further inland. This creates the need for different climate impact hazard communications for the public walkway and railway due to their cross-structure position on the same coastal infrastructure. Regular monitoring of the coastal wave climate, coastal water levels and seasonal beach levels provides early warning of an environmental state change and trends indicate the likely wave overtopping response to better prepare. Climate projections are often used to develop coastal resilience and adaptation plans to wave overtopping. Consideration of the more typical wave heights must be given otherwise there is large uncertainty in the annual hazard projection.

5. Conclusions

Concurrent metocean and wave overtopping field data allow improved understanding of the most common conditions that drive wave overtopping landward across the Dawlish sea wall for a full range of conditions. The study site represents a vertical beach fronted sea wall with large freeboard exposed to a bidirectional and bimodal wave climate. The meso-tidal regime exposes (dries) the structure toe at low tidal levels. We find in 1 year the following:

- 1. Most tides associated with overtopping (98% of the overtopping tides for the year 2021–2022) do not coincide with storms but typical wave sizes (1–1.5 m) that are common in the nearshore wave climate and less likely to be depth-limited during most high tides.
- 2. Future changes in the number of coastal wave overtopping events are likely to be controlled by the typical (moderate-sized but not large, i.e., 1–1.5 m at the structure) wave height category and their site-specific shallow water response to changes in climate, sea level and beach level.

 The prevailing wave direction observed in coastal monitoring is not the dominant direction associated with overtopping because it is associated with a wide spectrum of waves—the smallest and largest waves are unlikely to overtop.

- 4. The drivers causing a high number of wave overtopping events to reach different landward locations across the coastal structure differ, complicating (present and future) hazard communications.
- 5. An increase in water depth, due to sea-level rise and/or beach lowering, will affect coastal overtopping by waves of varying size differently. The overall change in the overtopping frequency distribution will be site-specific due to the complex balance in the non-linear dynamics of the wave spectrum to wave shoaling, breaking and reflection.

When investigating future overtopping hazard, it is critical to identify which wave heights contribute most to overtopping at a site due to the local wave, tide, beach-structure profile conditions and not focus on the (infrequent) extreme events only. Numerical assessments must consider wave overtopping by moderate waves to fully understand the cumulative annual hazard, the likely hazard duration over a tidal cycle and when in the tidal cycle overtopping is likely to be most frequent. Wave—depth and wave—current interactions should be investigated to fully understand the role of tidal asymmetries in controlling the wave overtopping hazard relative to predicted high tide.

Author Contributions: Conceptualization, J.B.; developing the methodology, J.B., M.Y. and G.M.; engineering bespoke instrumentation and equipment installations, R.P., D.J., C.C., J.W., B.M. and P.G.; fieldwork and data collection, R.P., D.J., C.C., J.W., B.M., P.G., J.S., T.P., C.S., M.Y. and J.B.; numerical model simulation, C.S.; data processing M.Y., T.P. and C.S.; formal analysis and discussion of information application, J.B., G.M., M.Y., J.G. and R.A.; investigation, J.B. and G.M.; writing—original draft preparation, J.B. and G.M.; writing—review and editing, M.Y., C.S., J.W., J.G. and R.A. All authors have read and agreed to the published version of the manuscript.

Funding: This research was funded by the Natural Environment Research Council (NERC), grant number NE/V002538/1 and NE/V002589/1.

Data Availability Statement: The data used in this research are available from the British Oceanographic Data Centre (https://www.bodc.ac.uk/data/published_data_library/catalogue/10.5285/12 ed58d6-7bb8-3eae-e063-6c86abc0689c/ (accessed on 21 August 2024)) and the National Network of Regional Coastal Monitoring Programmes of England (https://coastalmonitoring.org/ (accessed on 21 August 2024).

Acknowledgments: This research was completed through the project 'Coastal REsistance: Alerts and Monitoring Technologies (CreamT)' funded by NERC (NE/V002538/1; NE/V002589/1). Network Rail are thanked for their permission and support to install equipment at Dawlish. The WireWall overtopping datasets collected are now managed and were published by the British Oceanographic Data Centre (BODC), making them open access for others to use. Predicted high tides for Exmouth were computed and formatted by POLTIPS-3, the National Oceanography Centre's Tidal Software (https://noc-innovations.com/services/tide-prediction-software/coastal-software/ (accessed on 21 August 2024)). Their POLPRED package was used as a reference for the likely tidal currents. Coastal monitoring data (waves and water levels), collected by South West Coastal Monitoring (SWCM), were freely obtained from the National Network of Regional Coastal Monitoring Programmes (NNRCMP) of England. Tim Pullen at HR Wallingford Ltd. is recognised for his ongoing support and discussion about wave overtopping processes. Thomas Dhoop is thanked for sharing the wave rose plotting codes routinely used by the NNRCMP for reporting and for insights into tidal asymmetries seen within the wave climate along the south coast of England.

Conflicts of Interest: Author Julie Gregory was employed by the company Network Rail Wales & Western Region. The remaining authors declare that the research was conducted in the absence of any commercial or financial relationships that could be construed as a potential conflict of interest.

Appendix A. West Bay Wind Observations

The nearest wind observations available through the National Network of Regional Coastal Monitoring Programmes of England to the Dawlish study site are at West Bay (Figure A1a), a small harbour settlement with cliffs either side. The location is more open to offshore conditions than Dawlish, which at the study site is backed by a cliff with nearby coastal headlands creating sheltering. The wind climate (Figure A1b) at West Bay during the 1 year of wave overtopping monitoring (March 2021–2022) has a greater contribution from inland (NE, roughly aligned with the river) and alongshore (W) directions. Wind data from this location do not suggest that if more observations at Dawlish had been recorded (Figure 2e) there would have been more onshore conditions in that location during the study period. This station also stopped recording during Storm Barra (Section 3.2). The last data were logged 6 December 2021 23:50 and logging resumed 21 December 2021 10:30 (GMT).

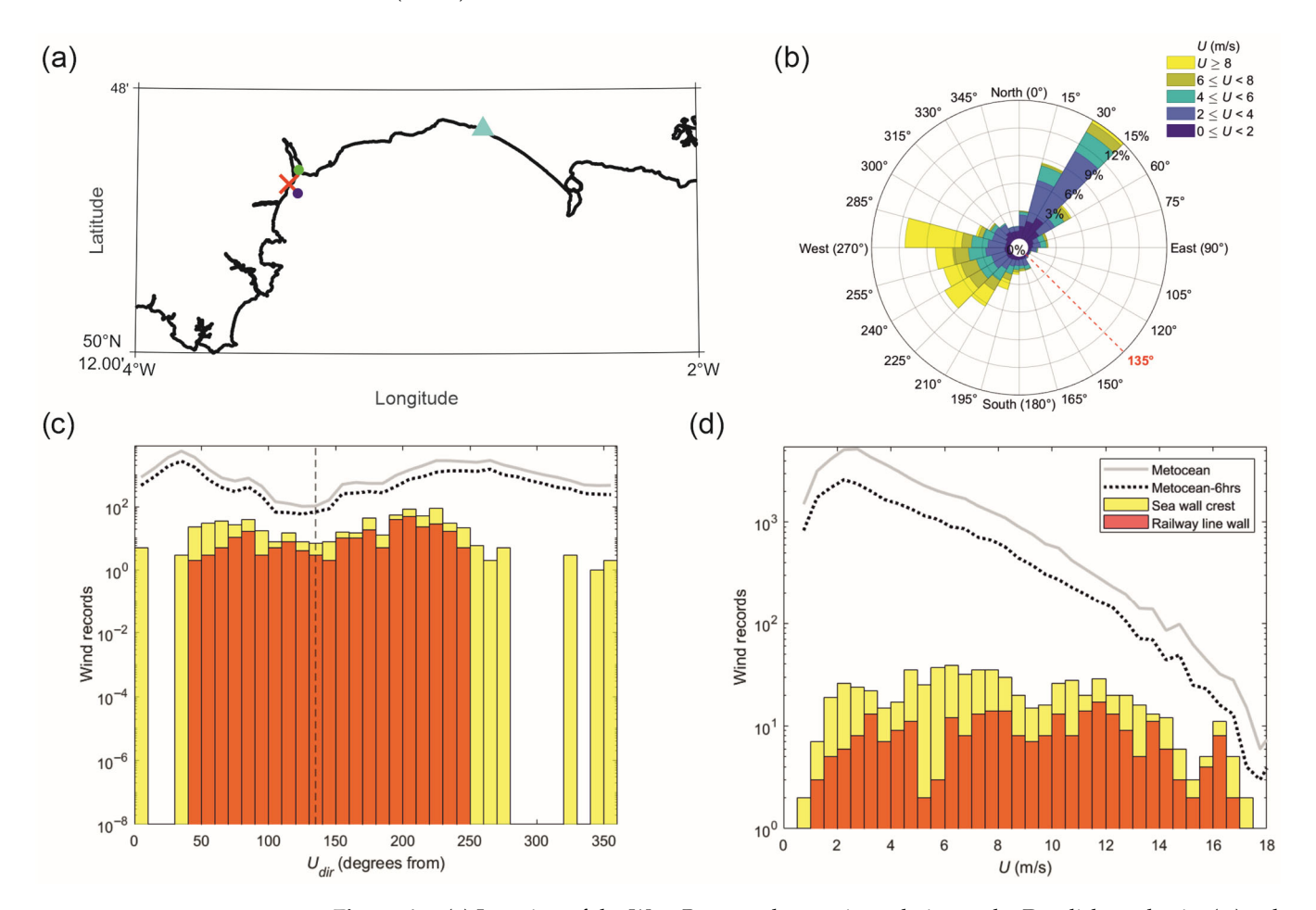


Figure A1. (a) Location of the West Bay weather station relative to the Dawlish study site (\triangle), other symbols are shown in Figure 1. (b) The West Bay wind rose. Histograms with log-y axis to show the number of observed records of metocean (MO) conditions and those conditions associated with wave overtopping at the sea wall crest (SC; yellow bars) and railway line wall (RW; orange bars). The metocean data are for the 1-year period (grey line) but the conditions compared with overtopping are limited to the 6 h high tide WireWall measurement window for every tide during the year (black dashed line). Wind observations were available at 10 min intervals for (c) wind direction, U_{dir} , (degrees), with the vertical dashed line indicating the onshore direction at Dawlish, not West Bay, and (d) wind speed, U, (m/s).

The data at West Bay are recorded at a 10 min interval as are the data specifically collected at Dawlish during the study. However, the data have not been combined to fill

gaps in monitoring (Figures 2e and 3g,h) due to the different topographic influence on the wind speeds and directions. When comparing the data, it is clear the West Bay station recorded a wider range of wind directions (Figure A1c) than in Dawlish (Figure 3g), with more frequent low wind speed conditions recorded and higher wind speeds (Figure A1d) than in Dawlish (Figure 3h). The general trend in wind direction associated with overtopping is similar, with bidirectional peaks occurring within 50° – 250° (Figure A1c). The stronger winds at West Bay most frequently occur from directions that would have an offshore component at Dawlish and locally the sea wall is likely to be sheltered by the cliff at the instrumented overtopping monitoring site.

References

- 1. Allsop, W.; Bruce, T.; Pearson, J.; Franco, L.; Burgin, J.; Ecob, C. Safety under wave overtopping—How overtopping processes and hazards are viewed by the public. *Coast. Eng.* **2005**, *4*, 4263–4274. [CrossRef]
- 2. Allsop, W.; Bruce, T.; Pearson, J.; Alderson, J.; Pullen, T. Violent wave overtopping at the coast, when are we safe? In *Proceedings of the Conference on Coastal Management*; Thomas Telford: London, UK, 2003; pp. 54–69.
- 3. Franco, L.; de Gerloni, M.; van der Meer, J. Wave overtopping on vertical and composite breakwaters. *Coast. Eng.* **1994**, 1030–1045. [CrossRef]
- 4. Garzon, J.L.; Ferreira, Ó.; Reis, M.T.; Ferreira, A.; Fortes, C.J.E.M.; Zózimo, A.C. Conceptual and quantitative categorization of wave-induced flooding impacts for pedestrians and assets in urban beaches. *Sci. Rep.* **2023**, *13*, 7251. [CrossRef]
- 5. Van der Meer, J.W.; Allsop, N.W.H.; Bruce, T.; De Rouck, J.; Kortenhaus, A.; Pullen, T.; Schüttrumpf, H.; Troch, P.; Zanuttigh, B. EurOtop. Manual on Wave Overtopping of Sea Defences and Related Structures. An Overtopping Manual Largely Based on European Research, but for Worldwide Application. 2018. Available online: https://www.overtopping-manual.com (accessed on 17 June 2025).
- 6. Salauddin, M.; O'Sullivan, J.J.; Abolfathi, S.; Peng, Z.; Dong, S.; Pearson, J.M. New insights in the probability distributions of wave-by-wave overtopping volumes at vertical breakwaters. *Sci. Rep.* **2022**, *12*, 16228. [CrossRef]
- 7. Jeong, J.; Barbosa, S.A.; Goodall, J.L. Quantifying the impact of nuisance flooding on urban coastal communities under present and future climatic conditions: Norfolk, Virginia as a case study. *J. Hydrol. Reg. Stud.* **2025**, *59*, 102304. [CrossRef]
- 8. Zahura, F.T.; Goodall, J.L.; Chen, T.D. Using crowdsourced data to estimate passenger vehicle travel delays from nuisance flooding. *Transp. Res. Part D Transp. Environ.* **2024**, 133, 104307. [CrossRef]
- 9. Almar, R.; Ranasinghe, R.; Bergsma, E.W.J.; Diaz, H.; Melet, A.; Papa, F.; Vousdoukas, M.; Athanasiou, P.; Dada, O.; Almeida, L.P.; et al. A global analysis of extreme coastal water levels with implications for potential coastal overtopping. *Nat. Commun.* **2021**, *12*, 3775. [CrossRef]
- 10. Rogers, J.S.; Maneta, M.P.; Sain, S.R.; Madaus, L.E.; Hacker, J.P. The role of climate and population change in global flood exposure and vulnerability. *Nat. Commun.* **2025**, *16*, 287. [CrossRef]
- 11. Allsop, W.; Bruce, T.; Pearson, J.; Besley, P. Wave overtopping at vertical and steep seawalls. *Marit. Eng.* **2005**, *158*, 103–114. [CrossRef]
- 12. Bruce, T.; Van der Meer, J.W.; Pullen, T.; Allsop, W. Wave overtopping at vertical and steep structures. In *Handbook of Coastal and Ocean Engineering*; World Scientific: Singapore, 2010; Chapter 16; pp. 411–439.
- 13. Cecioni, C.; Pepi, Y.; Franco, L. New 2D laboratory experiments on wave overtopping at vertical walls under impulsive and non-impulsive conditions. *Coast. Eng.* **2025**, *197*, 104689. [CrossRef]
- 14. Hames, D.P.; Vidal, I.; Gouldby, B.P. Impacts of sea level rise on wave overtopping rates around the coast of England. *Marit. Eng.* **2023**, *176*, 110–117. [CrossRef]
- 15. Stokes, K.; Poate, T.; Masselink, G.; King, E.; Saulter, A.; Ely, N. Forecasting coastal overtopping at engineered and naturally defended coastlines. *Coast. Eng.* **2021**, *164*, 103827. [CrossRef]
- Bagg, J.; Battley, M.; Whittaker, C.; Shand, T. Application of laboratory dam break experiments to non-impulsive wave overtopping. *Coast. Eng.* 2025, 198, 104695. [CrossRef]
- 17. Koosheh, A.; Etemad-Shahidi, A.; Cartwright, N.; Tomlinson, R.; van Gent, M. Individual wave overtopping at coastal structures: A critical review and the existing challenges. *Appl. Ocean Res.* **2021**, *106*, 102476. [CrossRef]
- 18. Van der Werf, I.M.; Van Gent, M.R.A. Wave Overtopping over Coastal Structures with Oblique Wind and Swell Waves. *J. Mar. Sci. Eng.* **2018**, *6*, 149. [CrossRef]
- de Santiago, I.; Plomaritis, T.A.; Avalos, D.; Garnier, R.; Abalia, A.; Epelde, I.; Liria, P. Comparison of wave overtopping estimation models for urban beaches. Towards an early warning system on the Basque coast. Sci. Total Environ. 2024, 912, 168783. [CrossRef]
- 20. Brown, J.M.; Yelland, M.J.; Masselink, G.; Poate, T.; Stokes, C.; Pascal, R.W.; Jones, D.S.; Cardwell, C.L.; Walk, J.; Martin, B.; et al. Coastal wave overtopping: New Nowcast and monitoring technologies. *Coast. Eng. Proc.* **2023**, *37*, papers.1. [CrossRef]

21. McGlade, M.; Valiente, N.G.; Brown, J.; Stokes, C.; Poate, T. Investigating appropriate artificial intelligence approaches to reliably predict coastal wave overtopping and identify process contributions. *Ocean Model.* **2025**, *194*, 102510. [CrossRef]

- 22. Lashley, C.; Brown, J.; Yelland, M.; van der Meer, J.; Pullen, T. Comparison of deep-water-parameter-based wave overtopping with wirewall field measurements and social media reports at Crosby (UK). *Coast. Eng.* **2023**, *179*, 104241. [CrossRef]
- 23. Pullen, T.; Allsop, W.; Bruce, T.; Pearson, J. Field and laboratory measurements of mean overtopping discharges and spatial distributions at vertical seawalls. *Coast. Eng.* **2009**, *56*, 121–140. [CrossRef]
- 24. Dong, S.; Abolfathi, S.; Salauddin, M.; Pearson, J.M. Spatial distribution of wave-by-wave overtopping behind vertical seawall with recurve retrofitting. *Ocean Eng.* **2021**, 238, 109674. [CrossRef]
- 25. Peng, Z.; Zou, Q.-P. Spatial distribution of wave overtopping water behind coastal structures. *Coast. Eng.* **2011**, *58*, 489–498. [CrossRef]
- 26. Yelland, M.J.; Brown, J.M.; Cardwell, C.L.; Jones, D.S.; Pascal, R.W.; Pinnell, R.; Pullen, T.; Silva, E. A system for in-situ, wave-by-wave measurements of the speed and volume of coastal overtopping. *Commun. Eng.* **2023**, *2*, 9. [CrossRef]
- 27. Pawlowicz, R. "M_Map: A Mapping Package for MATLAB", Version 1.4m [Computer Software]. 2020. Available online: www.eoas.ubc.ca/rich/map.html (accessed on 24 October 2024).
- 28. Scott, T.; Masselink, G.; Austin, M.J.; Russell, P. Controls on macrotidal rip current circulation and hazard. *Geomorphology* **2014**, 214, 198–215. [CrossRef]
- 29. Dawson, D.; Shaw, J.; Gehrels, W.R. Sea-level rise impacts on transport infrastructure: The notorious case of the coastal railway line at Dawlish, England. *J. Transp. Geogr.* **2016**, *51*, 97–109. [CrossRef]
- 30. NTSLF. POLTIPS, Tidal Prediction Software. Marine Data Products, National Tidal and Sea Level Facility 2021. Available online: https://ntslf.org/products/software (accessed on 14 July 2023).
- 31. Adams, K.; Heidarzadeh, M. A multi-hazard risk model with cascading failure pathways for the Dawlish (UK) railway using historical and contemporary data. *Int. J. Disaster Risk Reduct.* **2021**, *56*, 102082. [CrossRef]
- 32. Yelland, M.J.; Brown, J.M.; Pascal, R.W.; Jones, D.S.; Cardwell, C.L.; Walk, J.A.; Martin, B.; Darroch, L.; Gardner, T. Wave Overtopping Field Data Collected at the Sea Walls in Dawlish and Penzance (Southwest UK) Between March 2021 and March 2022. NERC EDS British Oceanographic Data Centre NOC, 12 April 2024. Available online: https://www.bodc.ac.uk/data/published_data_library/catalogue/10.5285/12ed58d6-7bb8-3eae-e063-6c86abc0689c (accessed on 12 April 2024).
- 33. Dhoop, T.; Thompson, C. Swell wave progression in the English Channel: Implications for coastal monitoring. *Anthr. Coasts* **2021**, 4, 281–305. [CrossRef]
- 34. Janssen, T.T.; Battjes, J.A. A note on wave energy dissipation over steep beaches. Coast. Eng. 2007, 54, 711–716. [CrossRef]
- 35. Pereira, D. Wind Rose, Online Resource. MATLAB Central File Exchange. Available online: https://www.mathworks.com/matlabcentral/fileexchange/47248-wind-rose (accessed on 14 February 2025).
- 36. Poate, T. Dawlish Wave Conditions, YouTube Video. 2023. 8th March 2022 Shown at 2:01 Minutes into the Clip. Available online: https://www.youtube.com/watch?v=DvJVQp_zL78 (accessed on 11 June 2025).
- 37. Davidson, M.A.; O'Hare, T.J.; George, K.J. Tidal modulation of incident wave heights: Fact or Fiction? *Reef J.* **2009**, *1*, 16–32. [CrossRef]
- 38. Thompson, D.A.; Karunarathna, H.; Reeve, D.E. Modelling Extreme Wave Overtopping at Aberystwyth Promenade. *Water* **2017**, 9, 663. [CrossRef]
- 39. Stein, L.P.; Siegle, E. Overtopping events on seawall-backed beaches: Santos Bay, SP, Brazil. Reg. Stud. Mar. Sci. 2020, 40, 101492. [CrossRef]
- 40. Briganti, R.; Musumeci, R.E.; van der Meer, J.; Romano, A.; Stancanelli, L.M.; Kudella, M.; Akbar, R.; Mukhdiar, R.; Altomare, C.; Suzuki, T.; et al. Wave overtopping at near-vertical seawalls: Influence of foreshore evolution during storms. *Ocean Eng.* 2022, 261, 112024. [CrossRef]
- 41. Xie, D.; Zou, Q.-P.; Mignone, A.; MacRae, J.D. Coastal flooding from wave overtopping and sea level rise adaptation in the northeastern USA. *Coast. Eng.* **2019**, *150*, 39–58. [CrossRef]

Disclaimer/Publisher's Note: The statements, opinions and data contained in all publications are solely those of the individual author(s) and contributor(s) and not of MDPI and/or the editor(s). MDPI and/or the editor(s) disclaim responsibility for any injury to people or property resulting from any ideas, methods, instructions or products referred to in the content.